Pharm Res (2014) 31:2429–2438
DOI 10.1007/s11095-014-1338-y

RESEARCH PAPER

Intracellular Ca^{2+} Release Mediates Cationic but Not Anionic Poly(amidoamine) (PAMAM) Dendrimer-Induced Tight Junction Modulation

Brittany R. Avaritt • Peter W. Swaan

Received: 15 January 2014 / Accepted: 8 February 2014 / Published online: 20 March 2014

ABSTRACT

Purpose Poly(amidoamine) (PAMAM) dendrimers show great promise for utilization as oral drug delivery vehicles. These polymers are capable of traversing epithelial barriers, and have been shown to translocate by both transcellular and paracellular routes. While many proof-of-concept studies have shown that PAMAM dendrimers improve intestinal transport, little information exists on the mechanisms of paracellular transport, specifically dendrimer-induced tight junction modulation.

Methods Using anionic G3.5 and cationic G4 PAMAM dendrimers with known absorption enhancers, we investigated tight junction modulation in Caco-2 monolayers by visualization and mannitol permeability and compared dendrimer-mediated tight junction modulation to that of established permeation enhancers. [^{14}C]-Mannitol permeability in the presence and absence of phospholipase C-dependent signaling pathway inhibitors was also examined and indicated that this pathway may mediate dendrimer-induced changes in permeability.

Results Differences between G3.5 and G4 in tight junction protein staining and permeability with inhibitors were evident, suggesting divergent mechanisms were responsible for tight junction modulation. These dissimilarities are further intimated by the intracellular calcium release caused by G4 but not G3.5. Based on our results, it is apparent that the underlying mechanisms of dendrimer permeability are complex, and the complexities are likely a result of the density and sign of the surface charges of PAMAM dendrimers.

Conclusions The results of this study will have implications on the future use of PAMAM dendrimers for oral drug delivery.

B. R. Avaritt • P. W. Swaan (✉)
Department of Pharmaceutical Sciences
Center for Nanomedicine and Cellular Drug Delivery
University of Maryland, Baltimore
20 Penn Street, Health Sciences Facility II, Room 543
Baltimore, Maryland 21201, USA
e-mail: pswaan@rx.umaryland.edu

KEY WORDS nanomedicine · oral drug delivery · PAMAM dendrimers · paracellular transport · tight junctions

INTRODUCTION

Poly (amidoamine) (PAMAM) dendrimers have been extensively investigated as potential drug delivery vehicles because they possess unique properties when compared to traditional polymers. Many of these properties result from the controlled synthesis of dendrimers leading to well-defined sizes, near monodispersity, and a controllable number of surface groups (1). The surface groups can be conjugated to drugs, imaging agents, and targeting moieties to create multifunctional nanocarriers (2,3). In addition to intravenous administration, several reports have suggested that PAMAM dendrimers can cross Caco-2 monolayers, a model of the intestinal epithelium (4–7). Conjugation or complexation of drugs with poor bioavailability to PAMAM dendrimers has successfully improved the permeability of these drugs *in vitro* (8–11); thus, PAMAM dendrimers show potential for oral drug delivery, which has many benefits over intravenous administration including a more flexible dosing regimen, increased convenience, better patient compliance, and lowered costs (12).

Mechanistically, dendrimers are transported across the epithelial barrier by both transcellular and paracellular pathways. We have previously shown that transport is energy dependent and reduced in the presence of both clathrin- and caveolin-mediated endocytosis inhibitors (13,14). Additionally, we showed that PAMAM dendrimers colocalize with markers for clathrin, early endosomes, and lysosomes, further establishing the mechanisms of dendrimer internalization and transcytosis (13,15). Dendrimers have also been shown to alter tight junction immunofluorescence and cause transient decreases in transepithelial electrical resistance (TEER) leading to suspected paracellular transport (7,13,16). While mechanisms of internalization are well established,

the mechanisms leading to tight junction modulation are largely unknown.

To elucidate possible mechanisms of tight junction modulation by dendrimers we can contrast their effects to the established permeation enhancers sodium caprate (C10) and ethylene glycol tetraacetic acid (EGTA), each with distinct mechanisms. C10 is a medium-chain fatty acid capable of increasing permeability through the phospholipase C (PLC)-dependent signaling pathway (17–19). In this pathway, phosphatidyl inositol (4,5)-bisphosphate (PIP_2) is cleaved by PLC into inositol 1,4,5-triphosphate (IP_3) and diacylglycerol (DAG) (20,21). IP_3 then causes calcium release from the endoplasmic reticulum, and the resulting increase in intracellular calcium activates protein kinase C (PKC) and calcium/calmodulin protein kinase II (CaMPKII) (22,23). Once activated, the protein kinases alter the activity of myosin light chain kinase (MLCK) leading to the phosphorylation of myosin light chain (MLC) (24). Incubation in calcium-free solutions with EGTA, a calcium chelator, also leads to increased MLCK activity (25). Changes in phosphorylation result in contraction of the perijunctional actomyosin ring and alteration of tight junction permeability (26).

For this study, we investigated the impact of both cationic and anionic PAMAM dendrimers on tight junctional assembly and function as well as the transport of the small paracellular permeability marker mannitol in fully differentiated Caco-2 monolayers. Additionally, a panel of inhibitors of the PLC-dependent signaling pathway was utilized in conjunction with calcium and MLC imaging to determine if dendrimers directly impact the pathway resulting in tight junction modulation. The results of this work will enhance the knowledge required for selecting dendrimers with appropriate charge and size for enhancing oral drug delivery.

MATERIALS AND METHODS

Materials

G3.5 and G4 PAMAM dendrimers, C10, EGTA, ML7, U73122, W7, and dynasore were purchased from Sigma Aldrich (St. Louis, MO). KN62, BAPTA-AM, and dioctanoylglycerol (diC8) were purchased from EMD Millipore (Billerica, MA). All cell culture supplies and antibodies were obtained from Life Technologies (Grand Island, NY) unless otherwise noted.

Cell Culture

The human colorectal adenocarcinoma cell line Caco-2 was obtained from the American Type Culture Collection (Manassas, VA). Cells (passages 20–40) were grown at 37°C with 5% CO_2 and 95% relative humidity. Cells were cultured in Dulbecco's modified Eagle's medium (DMEM) supplemented with 10% fetal bovine serum, 1% non-essential amino acids, 100 U/mL penicillin, and 10,000 μg/mL streptomycin. Media was changed every other day, and cells were passaged at 80–90% confluency using 0.25% trypsin/ethylene diamine tetraacetic acid (EDTA). For experiments, cells were seeded at 80,000 cells/well in 12-well polycarbonate Corning Transwell inserts with a 0.4 μm mean pore size (Corning, NY) and used after 21–28 days of growth. TEER was measured using a voltohmmeter (World Precision Instruments, Sarasota, FL) to assure proper monolayer formation, and monolayers with TEER > 500 $\Omega \cdot cm^2$ were used for experiments.

Tight Junction Immunofluorescence

Caco-2 monolayers were treated with Hank's balanced salt solution (HBSS) buffered with 10 mM 4-(2-Hydroxyethyl) piperazine-1-ethanesulfonic acid (HEPES), 0.01 or 0.1 mM G3.5, or 0.01 mM G4, since we have previously shown these concentrations to be non-cytotoxic (7,14). C10 and EGTA were also used at charge equivalent concentrations (0.64 mM and 0.16 mM, respectively) for comparison. Monolayers were treated for 2 h (30 min for EGTA). After treatment, the monolayers were washed twice in ice-cold HBSS, fixed for 30 min at 4°C with ethanol, and permeabilized with either 0.2% v/v Triton X-100 for 20 min at room temperature (actin, claudin-1, and ZO-1) or acetone for 1 min at −20°C (occludin). After blocking for 30 min at room temperature in 3% w/v bovine serum albumin (BSA) in Dulbecco's phosphate buffered saline (DPBS), monolayers were incubated with either rabbit anti-claudin-1 (8 μg/mL), rabbit anti-ZO-1 (2.5 μg/mL), or mouse anti-occludin (3 μg/mL) overnight at 4°C. The next morning, cells were washed with BSA solution and blocked for 30 min at room temperature. Alexa Fluor 568 goat anti-rabbit or anti-mouse IgG (1:400) was added to the monolayers for 1 h at room temperature. Monolayers stained for actin were incubated with rhodamine phalloidin for 20 min at room temperature. Once staining was complete, cells were washed with DPBS, and membranes were excised from the insert support. Membranes were mounted on glass slides with ProLong® Gold mounting medium containing DAPI. After curing at room temperature for 24 h, slides were sealed with clear nail polish and stored at 4°C until visualization.

Images were acquired using a Nikon A1 laser scanning confocal microscope. DAPI and AF568 were excited with 404 nm and 561 nm lasers, respectively, and 450/50 and 595/50 filter blocks were used for detection. Four z-stacks were acquired for each monolayer using the following parameters: Plan apo VC 60× oil objective, 33.33 μM pinhole, 4.6 μs pixel dwell, 2× line average, 2× optical zoom, 0.5 μM z-step size, and 512×512 image size. Images were then processed in Volocity 3D Image Analysis software v6.3 (PerkinElmer, Waltham, MA). Red voxels, corresponding to

tight junction staining, were quantified by thresholding the signal intensity between 20% and 100%. The number of red voxels for each treatment is compared to the HBSS control, and results are reported as the percentage increase in red voxels ± standard deviation (S.D.). Statistical significance was determined by using one-way analysis of variance (ANOVA) with Dunnett's test for multiple comparisons.

Tight Junction Protein Expression

Western blotting was used to measure claudin-1, occludin, and ZO-1 expression in Caco-2 monolayers after treatment for 1 or 2 h with 0.01 mM G4 and 0.01 mM, 0.1 mM, or 1 mM G3.5. After dendrimer treatment cells were washed twice with ice-cold HBSS buffer and lysed in RIPA buffer (50 mM Tris pH 8.0, 150 mM NaCl, 1.0% NP-40, 0.5% sodium deoxycholate, 0.1% SDS, 5 mM EDTA, 1 mM EGTA, 1 mM PMSF, protease inhibitor cocktail [Roche Applied Sciences, Indianapolis, IN]) for 30 min with gentle shaking at 4°C. Lysates were transferred to microcentrifuge tubes and cell debris was pelleted by centrifugation at 4°C for 2 min at 10,000×*g*. Total protein content of the supernatant was quantified by Bradford assay. Samples were prepared in Laemmli buffer (4% SDS, 20% glycerol, 10% 2-mercaptoethanol, 0.004% bromophenol blue, and 125 mM Tris HCl) to be 2 mg/mL total protein, and boiled for 5 min prior to separation by SDS-PAGE. Protein was loaded at 20 μg per well and separated using a 4–15% Tris–HCl gel (Bio-Rad, Hercules, CA) followed by overnight transfer to an Immobilon-FL membrane (EMD Millipore). After transfer, the membrane was blocked with 2% non-fat dry milk in Tris-buffered saline (TBS) for 1 h at 4°C. Membranes were then rinsed with TBS and incubated at 4°C overnight with primary antibody (1 μg/mL rabbit anti-claudin-1, 3 μg/mL rabbit anti-occludin, 3 μg/mL rabbit anti-ZO-1, 1 μg/mL mouse anti-calnexin) in TBS with 0.1% Tween-20 (TBST). Membranes were washed four times for 5 min each with TBST prior to incubation with secondary antibody (1:10,000 goat anti-rabbit IgG Dylight 800 and goat anti-mouse IgG Dylight 680 [KPL, Gaithersburg, MD]) in TBST for 45 min at room temperature. After incubation, the membrane was washed twice with TBST, followed by two TBS washes. Blots were imaged using an Odyssey infrared imaging system (Licor, Lincoln, NE), and densitometry analyses were performed using the Licor Image Studio software.

Dendrimer-Induced [^{14}C]-Mannitol Permeability

Transepithelial transport of [^{14}C]-mannitol was monitored in the apical to basolateral direction in differentiated Caco-2 monolayers in the presence or absence of 0.01 mM or 0.1 mM G3.5, 0.01 mM G4, 0.64 mM C10, or 0.16 mM EGTA. Cells were washed with HBSS supplemented with 10 mM HEPES, followed by treatment with dendrimers or permeation enhancers. Samples were taken at 1 and 2 h during treatment, and 1 and 2 h after treatment removal (3 and 4 h, respectively) from both the apical and basolateral compartments. At each time point, inserts were transferred to new wells containing fresh HBSS. Transport was quantified by scintillation counting. Mannitol permeability was measured again for 2 h without dendrimers 24 h after the initial treatment to monitor recovery.

Inhibition of Dendrimer-Mediated Tight Junction Modulation

Dendrimer-induced mannitol transport was again monitored in the apical to basolateral direction in differentiated Caco-2 monolayers with or without PLC signaling pathway inhibitors. [^{14}C]-mannitol permeability induced by either 1 mM G3.5 or 0.05 mM G4 was monitored in the presence of 10 μM U73122, 10 μM BAPTA-AM, 500 μM diC8, 40 μM W7, 10 μM KN62, 50 μM ML7, or 80 μM dynasore. Cells were pretreated with the inhibitors for 20 min at 37°C prior to the experiment. Samples were taken after a 2-h co-treatment of inhibitors and dendrimers. Mannitol permeability was also monitored with the inhibitors alone or with C10 as a positive control to insure the inhibitors did not interfere with marker permeability and were effective. Cytotoxicity studies were also performed using the WST-1 assay to ensure the inhibitors were nontoxic at the concentrations used. Permeability was determined by scintillation counting, and permeability in the presence of inhibitors was compared to standard dendrimer treatment controls. Results were analyzed using ANOVA with Dunnett's test for multiple comparisons.

Intracellular Calcium Release

Caco-2 cells were seeded onto collagen-coated chambered cover glass slides and grown for 21 days to form monolayers. Prior to treatment, cells were washed twice with HBSS buffer and incubated for 1 h at 37°C with dye loading buffer (2 μM Fluo-4 AM, 2.5 mM probenecid, and 20 mM HEPES in HBSS). After dye loading, cells were washed twice with wash solution (2.5 mM probenecid and 20 mM HEPES in HBSS) and then incubated at room temperature with either wash solution or wash solution containing 10 μM U73122 for 30 min. Dendrimer (0.01 mM G4; 0.01 mM, 0.1 mM, 1 mM G3.5) or calcium ionophore A23187 (2 μM) was added to cells during imaging. Live cells were imaged using a Nikon A1 confocal microscope fitted with an Okolab (Ottaviano, NA, Italy) Top Stage Incubator to maintain temperature and air/CO_2 ratio. Images were acquired using a 488 nm argon laser and a 525/50 filter with a 20× objective every 3 s for 10 min with a pixel dwell of 1 frame/s, a 22.8 μM pinhole,

and a 512×512 image size. The Nikon Perfect Focus System was used to compensate for focus drift. Fluorescence intensities for each time point were normalized to the baseline intensity obtained for each well before treatment addition and plotted *versus* time for comparison between treatments.

Phospho-Myosin Light Chain Immunofluorescence

Caco-2 monolayers were treated with either HBSS, 0.01 mM G4, 0.01 mM G3.5, or 0.1 mM G3.5 for 2 h or 1 mM EGTA for 15 min. After treatment, the monolayers were washed twice in ice-cold HBSS, fixed for 20 min at room temperature with 4% paraformaldehyde/4% sucrose in DPBS, washed twice with 25 mM glycine in DPBS, washed once with DBPS, and permeabilized with 0.2% v/v Triton X-100 for 20 min at room temperature. After rinsing three times with DBPS, cells were blocked for 30 min at room temperature in 3% BSA in DPBS. Monolayers were then incubated with 1:50 rabbit anti-phospho-myosin light chain 2 (Ser19) (Cell Signaling, Danvers, MA) overnight at 4°C. The next morning, cells were washed with the BSA solution and blocked for 30 min at room temperature. Alexa Fluor 488 goat anti-rabbit (1:500) was added to the monolayers for 1 h at room temperature. After washing three times with DBPS, monolayers were stained with rhodamine phalloidin (1:40) for 20 min at room temperature. Once staining was complete, cells were washed with DPBS, and membranes were excised from the insert support. Membranes were mounted on glass slides with ProLong Gold mounting medium containing DAPI. After curing at room temperature for 24 h, slides were sealed with clear nail polish and stored at 4°C until visualization.

Images were acquired similarly as described above for tight junction immunofluorescence. DAPI, AF488, and rhodamine were excited with 404 nm, 488 nm, and 561 nm lasers, respectively, and 450/50, 525/50 and 595/50 filter blocks were used for detection. Four z-stacks were acquired for each monolayer using the following parameters: Plan apo VC 60× oil objective, 33.33 μM pinhole, 4.6 μs pixel dwell, 2× line average, 3.5× optical zoom, 0.5 μM z-step size, and 512×512 image size.

RESULTS

Dendrimer-Induced Tight Junction Modulation

While the effect on actin and occludin staining in Caco-2 monolayers has been previously investigated for PAMAM dendrimers (7,13), we aimed to establish a comprehensive representation of tight junctional assembly by complementing these data with claudin-1 and ZO-1 staining; therefore, we assessed all four tight junction proteins upon treatment with dendrimers or absorption enhancers and compared the immunofluorescence to untreated cells (Fig. 1). For G4, no difference in staining occurred for actin, claudin-1, or occludin compared to the control; however, a slight increase was seen for ZO-1 staining indicating that tight junction modulation may have occurred. G3.5 also caused minimal differences in staining compared to control, with actin staining slightly decreased. In contrast, the higher concentration of G3.5 significantly increased staining of all proteins investigated. This effect has previously been associated with tight junction opening (7,13,16). For comparison, EGTA significantly increased staining and caused obvious retraction and redistribution of the tight junction proteins whereas C10 displayed no effect on the tight junctions at the concentration used.

To determine if the changes in tight junction staining with the dendrimers was caused by changes in protein expression, we used western blotting to quantify the proteins. Figure 2 shows the total expression of ZO-1, occludin, and claudin-1 during the same time frame in which the immunofluorescence study was conducted. Upon quantification and normalization to the calnexin loading control, no changes in protein expression were seen (data not shown). These results suggested that the increase in tight junction staining after dendrimer treatment was indeed a result of tight junction modulation and not changes in protein expression.

Since increased tight junction staining has been associated with tight junction opening and increased paracellular permeability (7), we examined mannitol transport in the presence of the dendrimers and absorption enhancers. Mannitol transport is a well-established method for monitoring changes in monolayer permeability (27). We measured [^{14}C]-mannitol permeability at 1 and 2 h during dendrimer and absorption enhancer treatment, removed the treatment, and continued to measure permeability for an additional 2 h (Fig. 3). At the concentrations used, neither G3.5 nor C10 increased mannitol permeability. For G4, an increase in permeability occurred gradually over the first 2 h, and the increased permeability continued for an hour after the dendrimer was removed before recovery began. EGTA displayed the largest increase in mannitol permeability, and, unlike G4, recovery began as soon as the EGTA was removed and calcium was reintroduced to the monolayers. After the initial treatments, the monolayers were maintained in cell culture medium for 24 h. Mannitol permeability was repeated after the monolayer recovery period, and the G4- and EGTA-induced permeability increase was shown to be completely reversible.

Inhibition of Dendrimer-Mediated Tight Junction Modulation

Because G3.5 and G4 displayed divergent results in tight junction staining and mannitol permeability, we aimed to

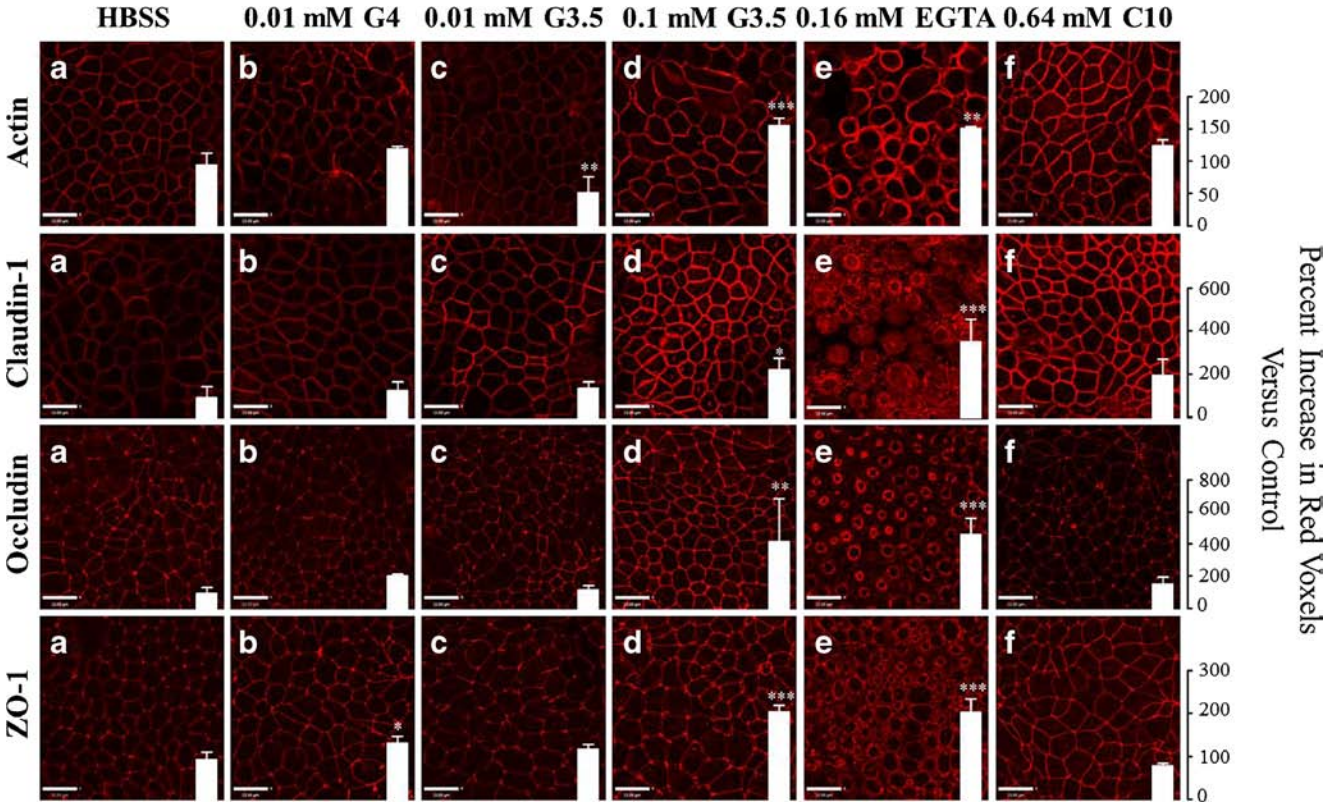

Fig. 1 Actin, claudin-1, occludin, and ZO-1 immunofluorescence in differentiated Caco-2 monolayers. Protein staining was visualized after a 2-h treatment (30 min for EGTA) with HBSS (**a**), 0.01 mM G4 (**b**), 0.01 mM G3.5 (**c**), 0.1 mM G3.5 (**d**), 0.16 mM EGTA (**e**), or 0.64 mM C10 (**f**). Quantification of tight junction staining is overlaid. Results are reported as the percentage of red voxels per region as compared to the untreated control ± standard deviation (S.D.) ($n = 3$). *, **, and *** denote a statistically significant increase in voxel count relative to the HBSS control with $p < 0.05$, $p < 0.01$, and $p < 0.001$, respectively. *Scale bar* = 10 μM.

establish possible mechanisms for dendrimer-induced tight junction modulation by investigating the effects of dendrimers on the PLC signaling pathway. A panel of biochemical inhibitors and known pathway modulators were co-incubated with either G3.5 or G4 to determine changes in dendrimer-induced mannitol permeability. For clarity, Fig. 4 illustrates specific points in the pathway where each individual inhibitor/modulator used in these studies exerts an effect. U73122, a PLC inhibitor that prevents the hydrolysis of PIP_2 into IP_3 and DAG (28), caused no change in permeability induced by G3.5 and G4. The calcium chelator BAPTA, which reduces intracellular calcium, also had no effect on

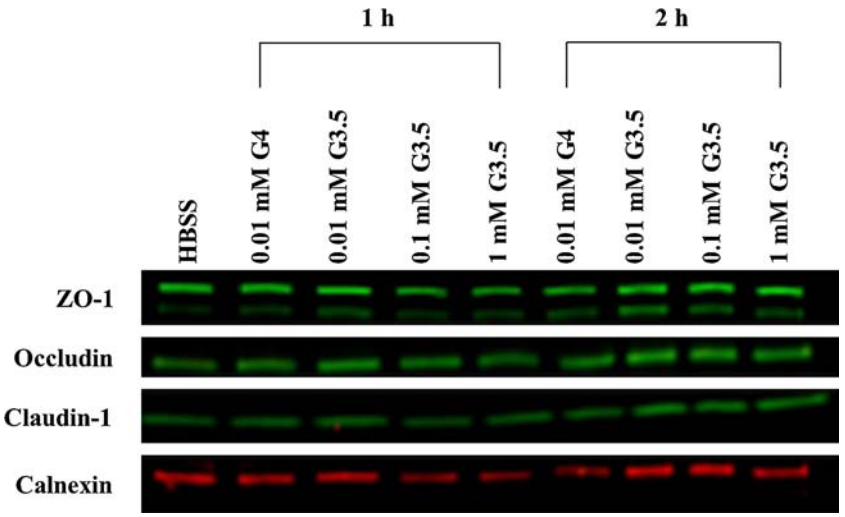

Fig. 2 Tight junction protein expression after treatment with HBSS only, 0.01 mM G4, 0.1 mM G3.5, and 1 mM G3.5 after 1 and 2 h. Calnexin was used as a loading control.

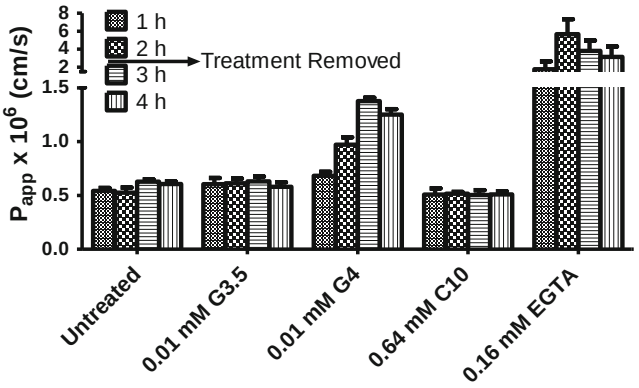

Fig. 3 Apparent permeability of [^{14}C]-mannitol during and immediately following treatment of Caco-2 monolayers with dendrimers or absorption enhancers. Mean ± S.D. ($n = 3$).

the activity of the dendrimers. For the IP_3 pathway inhibitors, varying results were seen. W7, a calcium/calmodulin antagonist (29), did not have an effect on dendrimer-induced permeability. The CaMPKII inhibitor KN62 (30) significantly decreased dendrimer-induced permeability for G3.5 but not G4. For ML7, a MLCK inhibitor that prevents the phosphorylation of MLC (31), the dendrimers exhibited different effects; G3.5 had no change in [^{14}C]-mannitol permeability while G4 imparted a significant permeability increase. The apparent increase in G4-induced permeability was not, however, a result of tight junction opening but of synergistic toxicity that occurred when ML7 and G4 were co-administered. Inclusion of the DAG analog diC8 (32) had no effect on dendrimer permeability. Taken together, these results shown in Fig. 5 suggest that dendrimer-induced tight junction modulation is not entirely mediated through PLC-dependent mechanisms. The endocytosis inhibitor dynasore, which inhibits dynamin 1 and dynamin 2 GTPases responsible for vesicle scission (33), was also included in the study because previous research demonstrated the importance of endocytosis for G3.5-mediated tight junction modulation (13). As expected, a significant decrease in G3.5-induced mannitol permeability occurred; however, dynasore had no influence on G4-induced permeability. Therefore, surface charge impacts the tight junction modulating ability of PAMAM dendrimers, and endocytosis plays an important role in tight junction modulation for anionic but not cationic dendrimers.

Intracellular Calcium Release During Dendrimer Treatment

To further investigate the role of calcium in dendrimer-induced tight junction modulation, the calcium sensitive fluorophore Fluo-4 AM was used to monitor calcium release upon dendrimer treatment. Addition of G3.5 up to 1 mM had no effect on intracellular calcium (Fig. 6a). G4, however, caused an immediate release of calcium and increase in fluorescence intensity. Figure 6b shows an initial calcium release followed by a period of calcium puffs. The response continued during the timeframe of cell imaging (10 min). To determine if the calcium release was associated with the PLC pathway, U73122 was used to inhibit the pathway. After incubation with this inhibitor, G4-induced calcium release was eliminated, indicating that the initial response was associated with the PLC pathway. The calcium ionophore A23187 was used as a positive control, and the effect of the ionophore was not altered by U73122 treatment.

Myosin Light Chain Phosphorylation

MLC plays an important role in tight junction modulation, and phosphorylation of MLC leads to the contraction of the perijunctional actomyosin ring (26). Since the MLCK inhibitor ML7 displayed varying results between G3.5 and G4, we aimed to further explore the potential role of MLC in dendrimer-induced tight junction changes by examining immunofluorescence of phospho-MLC. Neither G3.5 nor G4 showed any increase in phospho-MLC

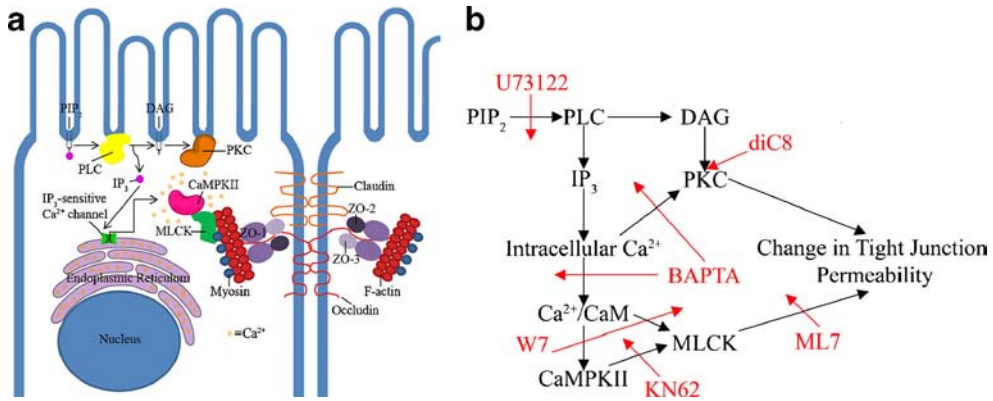

Fig. 4 PLC-dependent signaling pathway regulating changes in tight junction permeability (**a**), and investigated sites of inhibition (**b**).

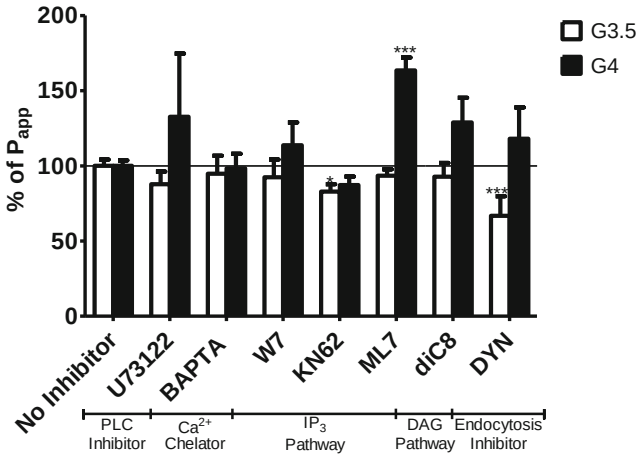

Fig. 5 Percent of apparent permeability of [^{14}C]-mannitol compared to uninhibited control for G3.5 (*white bars*) or G4 (*black bars*) treatment in Caco-2 monolayers. Mean ± S.D. ($n=6$). * and *** denote a statistically significant change in P_{app} compared to no inhibitor with $p<0.05$ and $p<0.001$, respectively.

compared to the untreated control (Fig. 7), indicating that MLC phosphorylation was not likely responsible for dendrimer-induced tight junction modulation. EGTA was used as a positive control and displayed a significant increase in MLC phosphorylation.

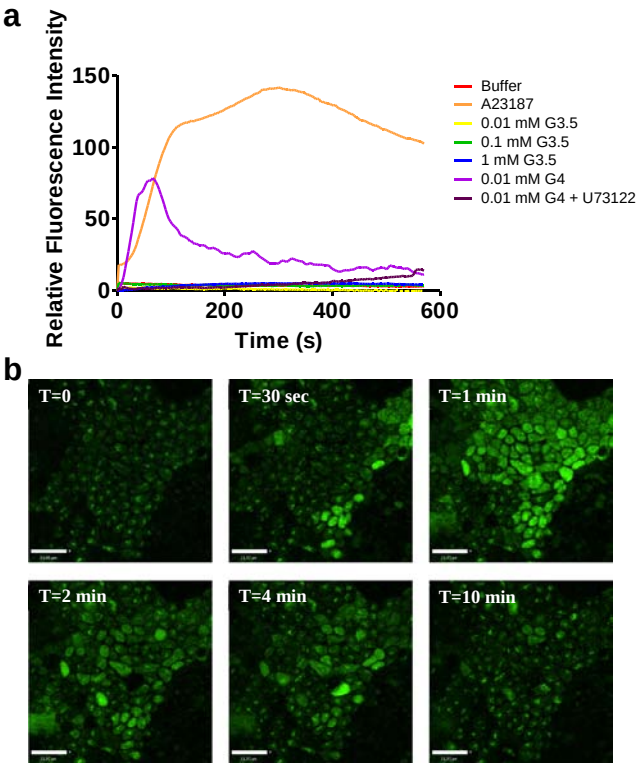

Fig. 6 Relative Fluo-4 fluorescence intensity upon dendrimer and control treatment (**a**), and time lapsed images during G4 treatment (**b**). Images were obtained every 3 s for 10 min, and the fluorescence intensity was normalized to the untreated control. *Scale bar* = 21 μm.

DISCUSSION

Previous studies have shown that PAMAM dendrimers hold promise as oral drug delivery vehicles for poorly bioavailable drugs as evidenced by the ability of dendrimer-drug conjugates to traverse the gut epithelium (8–11). Dendrimer-induced tight junction modulation has been the speculative cause of increased permeability to this point, and both anionic and cationic PAMAM dendrimers are thought to be capable of modulating tight junctions (6). In this work we have elucidated potential mechanisms for PAMAM dendrimer-mediated tight junction modulation. For our studies, we focused on comparing dendrimers of similar size with opposite surface charge. We also compared these dendrimers to known absorption enhancers to ascertain that PAMAM dendrimers act as potent tight junction modulators. The medium-chain fatty acid C10 and the calcium chelator EGTA were used because both have well established tight junction modulation mechanisms (17,25).

We compared tight junction protein staining and mannitol transport in Caco-2 monolayers treated with either dendrimers or permeation enhancers. Charge equivalent concentrations were chosen for comparison because the dendrimers' transport properties are largely imparted by their relative charge density. By visualizing tight junction proteins, we recorded the direct effect dendrimers had on supramolecular junctional assembly. For G4, only ZO-1 displayed increased staining. G3.5 showed decreased actin staining for the lower concentration but significant staining for all tight junction proteins at the higher (non-cytotoxic) concentration tested in this study, suggesting tight junction modulation. Tight junction visualization, however, was contradictory to the mannitol permeability results in which G4 but not G3.5 allowed for increased transport. Increased tight junction staining has been assumed to indicate enhanced tight junction protein accessibility and opening (7,13,16). Our results indicated that the increased fluorescence did not correlate with the ability to allow for small molecule paracellular transport and suggested that this method was not an appropriate indicator of tight junction opening. In fact, the observed increase in immunofluorescence was more likely a result of tight junction protein redistribution rather than tight junction opening. Increased ZO-1 staining in the case of G4 may be indicative of recruitment of the protein to the tight junctions. ZO-1 serves several roles within the cell in addition to supporting the tight junction scaffolding (34,35), and recruitment of ZO-1 to the tight junctions may allow for tight junction opening induced by G4 treatment (36,37). The decrease in actin staining for 0.01 mM G3.5 may be a result of dendrimer-induced depolymerization of the actin before restructuring of the tight junctions. At the higher concentration, the G3.5-induced restructuring occurred quicker, and the result was an increased amount of tight junction proteins at the cell–cell

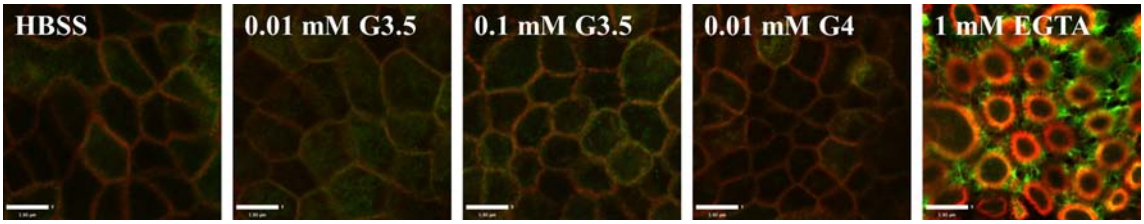

Fig. 7 Phospho-MLC immunofluorescence in Caco-2 monolayers. Staining was visualized after a 2-h treatment with HBSS, 0.01 mM G4, 0.01 mM G3.5, 0.1 mM G3.5, or 1 mM EGTA (30 min treatment). *Green* = phospho-MLC, *red* = actin. *Scale bar* = 5.9 μM.

interface at the time of staining. Similar results were seen for capsaicin, which opened tight junctions through mechanisms independent of MLCK (38).

To further delineate the mechanism behind dendrimer-mediated tight junction modulation, we used a panel of inhibitors and modulators of the PLC-dependent signaling pathway. Of the compounds used, only KN62 and ML7 affected dendrimer-induced mannitol transport. For G3.5, KN62 decreased transport. KN62 is a CaMPKII inhibitor that blocks the phosphorylation of MLCK by interacting with the calmodulin-binding site of CaMPKII (30). G4-induced transport increased with co-incubation of ML7. The increase in transport caused by inhibiting MLC phosphorylation was not the result of dendrimer-induced tight junction opening but of increased cell death that occurred. Individually, neither ML7 nor G4 were cytotoxic at the concentrations used; however, when combined a significant decrease in cell viability occurred. Because MLC is responsible for shuttling proteins to their cellular destinations (39), using ML7 may result in changes to the normal milieu of cell membrane components making the membrane more susceptible to the large positive charge of the cationic dendrimer which is known to interact with cells electrostatically (40). MLC is also responsible for membrane turnover to recover cell volume after osmotic stress, which the cell would not be able to overcome when ML7 is present (41). More studies are required to determine the cause of the synergistic toxicity induced by G4 and ML7.

In addition to PLC pathway inhibitors, dynasore was used to determine the effect of endocytosis on dendrimer-mediated tight junction modulation. Previous work showed that internalization of G3.5 was necessary for increased tight junction staining (13). In our study, dynasore treatment significantly decreased G3.5-induced mannitol transport, further supporting the requirement of internalization prior to tight junction modulation. G4-induced mannitol transport, however, was not affected by dynasore; therefore, dynamin-mediated endocytosis was not required for tight junction modulation. Cationic dendrimers may still internalize through other mechanisms such as macropinocytosis (42); thus, internal interactions leading to tight junction modulation cannot be ruled out.

Our observation that KN62 decreased G3.5-induced mannitol transport combined with previous reports hypothesizing that PAMAM dendrimers may behave like calcium chelators to open tight junctions (6,7) prompted us to investigate intracellular calcium release and MLC phosphorylation. Up to 1 mM G3.5 had no effect on intracellular calcium; however, G4 caused immediate calcium release (Fig. 6). After the initial release, calcium puffs continued for up to 10 min. In comparison, the calcium ionophore A23187 caused a sustained increase in calcium release (Fig. 6). Preincubation with U73122 eliminated G4-induced calcium release but not calcium release resulting from ionophore treatment, suggesting that G4 calcium modulation was associated with the PLC-dependent signaling pathway. Although this result appears contradictory to inhibition studies in which neither U73122 nor BAPTA affected G4-induced mannitol transport (Fig. 5), it should be noted that mannitol transport was investigated after a 2-h incubation whereas calcium release was visualized instantaneously. Future studies with shorter incubation periods and higher BAPTA concentrations to buffer the effect of G4-stimulated calcium release may be required to possibly demonstrate a potential association with the PLC pathway. We further investigated MLC phosphorylation to determine whether PAMAM dendrimers modulate tight junctions through alterations in MLC activity similar to EGTA; however, neither G3.5 nor G4 elicited any effect on MLC phosphorylation (Fig. 7).

Our results demonstrate that significant differences exist between anionic and cationic dendrimers' ability to modulate tight junctions. Anionic dendrimers show little effect on tight junctions or the pathway(s) associated with their regulated opening and closing; however, cationic dendrimers open tight junctions for small molecule transport by releasing intracellular calcium stores and increasing calcium signaling. The high uptake and transport properties previously seen for G3.5 (6) were likely due to the efficient endocytosis mechanisms by which the dendrimer is internalized (13) and *not* a result of paracellular transport of the dendrimer itself. G4 is more likely to be transported both by transcellular and paracellular mechanisms because of the effect on calcium signaling and nonspecific cell membrane association. Additional studies are

warranted to further explore the molecular mechanisms behind the observed G4-mediated epithelial permeation enhancement.

CONCLUSION

In this work we reported a possible mechanism of paracellular transport and tight junction modulation by PAMAM dendrimers in differentiated Caco-2 monolayers. We found that despite previous reports (4,6,7,16), G3.5 did not open tight junctions, whereas G4 modulated tight junctions to allow for paracellular transport of mannitol. The mechanism by which G4 modulates tight junctions was in part associated with the PLC-dependent signaling pathway; however, the charge density of the dendrimer likely allows for additional intracellular interactions that have yet to be unraveled. To fully harness the potential of dendrimers as oral drug delivery vehicles we must first understand the underlying mechanisms of dendrimer transport properties. The current study provides new insights in dendrimer-mediated tight junction modulation and may aid in the selection of dendrimers with tailored properties amenable to drug-specific oral delivery.

ACKNOWLEDGMENTS AND DISCLOSURES

Financial support was provided in part by an American Foundation for Pharmaceutical Education predoctoral fellowship to B. Avaritt. Dr. Jason Hill and Dr. Andrew Ziman provided guidance with live intracellular calcium imaging studies.

REFERENCES

1. Esfand R, Tomalia DA. Poly(amidoamine) (PAMAM) dendrimers: from biomimicry to drug delivery and biomedical applications. Drug Discov Today. 2001;6:427–36.
2. Tomalia DA, Reyna LA, Svenson S. Dendrimers as multi-purpose nanodevices for oncology drug delivery and diagnostic imaging. Biochem Soc Trans. 2007;35:61–7.
3. Kaminskas LM, Boyd BJ, Porter CJ. Dendrimer pharmacokinetics: the effect of size, structure and surface characteristics on ADME properties. Nanomedicine. 2011;6:1063–84.
4. El-Sayed M, Ginski M, Rhodes C, Ghandehari H. Transepithelial transport of poly(amidoamine) dendrimers across Caco-2 cell monolayers. J Control Release. 2002;81:355–65.
5. El-Sayed M, Rhodes CA, Ginski M, Ghandehari H. Transport mechanism(s) of poly (amidoamine) dendrimers across Caco-2 cell monolayers. Int J Pharm. 2003;265:151–7.
6. Kitchens KM, El-Sayed ME, Ghandehari H. Transepithelial and endothelial transport of poly (amidoamine) dendrimers. Adv Drug Deliv Rev. 2005;57:2163–76.
7. Kitchens KM, Kolhatkar RB, Swaan PW, Eddington ND, Ghandehari H. Transport of poly(amidoamine) dendrimers across Caco-2 cell monolayers: influence of size, charge and fluorescent labeling. Pharm Res. 2006;23:2818–26.
8. Goldberg DS, Vijayalakshmi N, Swaan PW, Ghandehari H. G3.5 PAMAM dendrimers enhance transepithelial transport of SN38 while minimizing gastrointestinal toxicity. J Control Release. 2011;150:318–25.
9. Kolhatkar RB, Swaan P, Ghandehari H. Potential oral delivery of 7-ethyl-10-hydroxy-camptothecin (SN-38) using poly(amidoamine) dendrimers. Pharm Res. 2008;25:1723–9.
10. Sadekar S, Thiagarajan G, Bartlett K, Hubbard D, Ray A, McGill LD, *et al.* Poly(amido amine) dendrimers as absorption enhancers for oral delivery of camptothecin. Int J Pharm. 2013;456:175–85.
11. Thiagarajan G, Ray A, Malugin A, Ghandehari H. PAMAM-camptothecin conjugate inhibits proliferation and induces nuclear fragmentation in colorectal carcinoma cells. Pharm Res. 2010;27:2307–16.
12. Banna GL, Collova E, Gebbia V, Lipari H, Giuffrida P, Cavallaro S, *et al.* Anticancer oral therapy: emerging related issues. Cancer Treat Rev. 2010;36:595–605.
13. Goldberg DS, Ghandehari H, Swaan PW. Cellular entry of G3.5 poly (amido amine) dendrimers by clathrin- and dynamin-dependent endocytosis promotes tight junctional opening in intestinal epithelia. Pharm Res. 2010;27:1547–57.
14. Kitchens KM, Kolhatkar RB, Swaan PW, Ghandehari H. Endocytosis inhibitors prevent poly(amidoamine) dendrimer internalization and permeability across Caco-2 cells. Mol Pharm. 2008;5:364–9.
15. Kitchens KM, Foraker AB, Kolhatkar RB, Swaan PW, Ghandehari H. Endocytosis and interaction of poly (amidoamine) dendrimers with Caco-2 cells. Pharm Res. 2007;24:2138–45.
16. Sweet DM, Kolhatkar RB, Ray A, Swaan P, Ghandehari H. Transepithelial transport of PEGylated anionic poly(amidoamine) dendrimers: implications for oral drug delivery. J Control Release. 2009;138:78–85.
17. Lindmark T, Schipper N, Lazorova L, de Boer AG, Artursson P. Absorption enhancement in intestinal epithelial Caco-2 monolayers by sodium caprate: assessment of molecular weight dependence and demonstration of transport routes. J Drug Target. 1998;5:215–23.
18. Tomita M, Hayashi M, Awazu S. Absorption-enhancing mechanism of EDTA, caprate, and decanoylcarnitine in Caco-2 cells. J Pharm Sci. 1996;85:608–11.
19. Tomita M, Hayashi M, Awazu S. Absorption-enhancing mechanism of sodium caprate and decanoylcarnitine in Caco-2 cells. J Pharmacol Exp Ther. 1995;272:739–43.
20. Berridge MJ, Dawson RM, Downes CP, Heslop JP, Irvine RF. Changes in the levels of inositol phosphates after agonist-dependent hydrolysis of membrane phosphoinositides. Biochem J. 1983;212:473–82.
21. Streb H, Irvine RF, Berridge MJ, Schulz I. Release of Ca2+ from a nonmitochondrial intracellular store in pancreatic acinar cells by inositol-1,4,5-trisphosphate. Nature. 1983;306:67–9.
22. Jaken S. Protein kinase C isozymes and substrates. Curr Opin Cell Biol. 1996;8:168–73.
23. Schulman H. The multifunctional Ca2+/calmodulin-dependent protein kinases. Curr Opin Cell Biol. 1993;5:247–53.
24. Turner JR, Angle JM, Black ED, Joyal JL, Sacks DB, Madara JL. PKC-dependent regulation of transepithelial resistance: roles of MLC and MLC kinase. Am J Physiol. 1999;277:C554–62.
25. Ma TY, Tran D, Hoa N, Nguyen D, Merryfield M, Tarnawski A. Mechanism of extracellular calcium regulation of intestinal epithelial tight junction permeability: role of cytoskeletal involvement. Microsc Res Tech. 2000;51:156–68.
26. Cunningham KE, Turner JR. Myosin light chain kinase: pulling the strings of epithelial tight junction function. Ann N Y Acad Sci. 2012;1258:34–42.
27. Ghandehari H, Smith PL, Ellens H, Yeh PY, Kopecek J. Size-dependent permeability of hydrophilic probes across rabbit colonic epithelium. J Pharmacol Exp Ther. 1997;280:747–53.

28. Smith RJ, Sam LM, Justen JM, Bundy GL, Bala GA, Bleasdale JE. Receptor-coupled signal transduction in human polymorphonuclear neutrophils: effects of a novel inhibitor of phospholipase C-dependent processes on cell responsiveness. J Pharmacol Exp Ther. 1990;253:688–97.
29. Hidaka H, Sasaki Y, Tanaka T, Endo T, Ohno S, Fujii Y, *et al.* N-(6-aminohexyl)-5-chloro-1-naphthalenesulfonamide, a calmodulin antagonist, inhibits cell proliferation. Proc Natl Acad Sci U S A. 1981;78:4354–7.
30. Tokumitsu H, Chijiwa T, Hagiwara M, Mizutani A, Terasawa M, Hidaka H. KN-62, 1-[N, O-bis(5-isoquinolinesulfonyl)-N-methyl-L-tyrosyl]-4-phenylpiperazi ne, a specific inhibitor of Ca2+/calmodulin-dependent protein kinase II. J Biol Chem. 1990;265:4315–20.
31. Saitoh M, Ishikawa T, Matsushima S, Naka M, Hidaka H. Selective inhibition of catalytic activity of smooth muscle myosin light chain kinase. J Biol Chem. 1987;262:7796–801.
32. Balda MS, Gonzalez-Mariscal L, Matter K, Cereijido M, Anderson JM. Assembly of the tight junction: the role of diacylglycerol. J Cell Biol. 1993;123:293–302.
33. Macia E, Ehrlich M, Massol R, Boucrot E, Brunner C, Kirchhausen T. Dynasore, a cell-permeable inhibitor of dynamin. Dev Cell. 2006;10:839–50.
34. Bauer H, Zweimueller-Mayer J, Steinbacher P, Lametschwandtner A, Bauer HC. The dual role of zonula occludens (ZO) proteins. J Biomed Biotechnol. 2010;2010:402593.
35. Farkas AE, Capaldo CT, Nusrat A. Regulation of epithelial proliferation by tight junction proteins. Ann N Y Acad Sci. 2012;1258:115–24.
36. Balda MS, Matter K. The tight junction protein ZO-1 and an interacting transcription factor regulate ErbB-2 expression. EMBO J. 2000;19:2024–33.
37. Fanning AS, Van Itallie CM, Anderson JM. Zonula occludens-1 and -2 regulate apical cell structure and the zonula adherens cytoskeleton in polarized epithelia. Mol Biol Cell. 2012;23:577–90.
38. Nagumo Y, Han J, Bellila A, Isoda H, Tanaka T. Cofilin mediates tight-junction opening by redistributing actin and tight-junction proteins. Biochem Biophys Res Commun. 2008;377:921–5.
39. DePina AS, Langford GM. Vesicle transport: the role of actin filaments and myosin motors. Microsc Res Tech. 1999;47:93–106.
40. Tiriveedhi V, Kitchens KM, Nevels KJ, Ghandehari H, Butko P. Kinetic analysis of the interaction between poly(amidoamine) dendrimers and model lipid membranes. Biochim Biophys Acta. 2011;1808:209–18.
41. Barfod ET, Moore AL, Van de Graaf BG, Lidofsky SD. Myosin light chain kinase and Src control membrane dynamics in volume recovery from cell swelling. Mol Biol Cell. 2011;22:634–50.
42. Albertazzi L, Serresi M, Albanese A, Beltram F. Dendrimer internalization and intracellular trafficking in living cells. Mol Pharm. 2010;7:680–8.